

Understanding the Interaction of Block Copolymers with DMPC Lipid Bilayer using Coarse-Grained Molecular Dynamics Simulations

Samira Hezaveh, Susruta Samanta, Antonio De Nicola, Giuseppe Milano, and Danilo Roccatano

J. Phys. Chem. B, **Just Accepted Manuscript** • Publication Date (Web): 08 Nov 2012

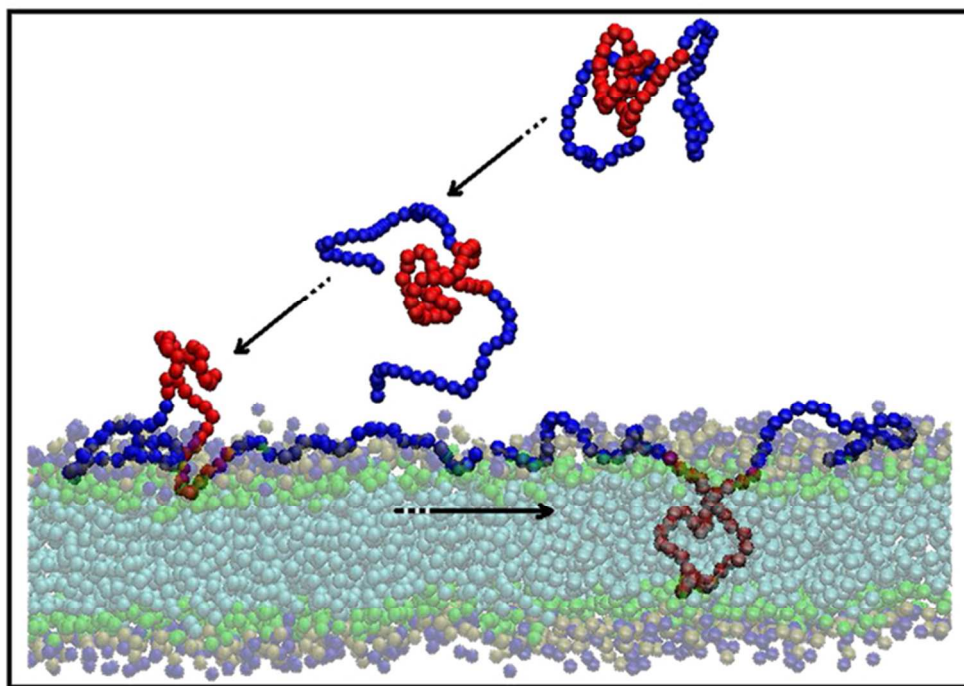
Downloaded from <http://pubs.acs.org> on November 14, 2012

Just Accepted

“Just Accepted” manuscripts have been peer-reviewed and accepted for publication. They are posted online prior to technical editing, formatting for publication and author proofing. The American Chemical Society provides “Just Accepted” as a free service to the research community to expedite the dissemination of scientific material as soon as possible after acceptance. “Just Accepted” manuscripts appear in full in PDF format accompanied by an HTML abstract. “Just Accepted” manuscripts have been fully peer reviewed, but should not be considered the official version of record. They are accessible to all readers and citable by the Digital Object Identifier (DOI®). “Just Accepted” is an optional service offered to authors. Therefore, the “Just Accepted” Web site may not include all articles that will be published in the journal. After a manuscript is technically edited and formatted, it will be removed from the “Just Accepted” Web site and published as an ASAP article. Note that technical editing may introduce minor changes to the manuscript text and/or graphics which could affect content, and all legal disclaimers and ethical guidelines that apply to the journal pertain. ACS cannot be held responsible for errors or consequences arising from the use of information contained in these “Just Accepted” manuscripts.



1
2
3
4
5
6
7
8
9
10
11
12
13
14
15
16
17
18
19
20
21
22
23
24
25
26
27
28
29
30
31
32
33
34
35
36
37
38
39
40
41
42
43
44
45
46
47
48
49
50
51
52
53
54
55
56
57
58
59
60



60x43mm (300 x 300 DPI)

1
2
3
4
5
6
7
8
9
10
11
12
13
14
15
16
17
18
19
20
21
22
23
24
25
26
27
28
29
30
31
32
33
34
35
36
37
38
39
40
41
42
43
44
45
46
47
48
49
50
51
52
53
54
55
56
57
58
59
60

Understanding the Interaction of Block Copolymers with DMPC Lipid Bilayer Using Coarse-Grained Molecular Dynamics Simulations

Samira Hezaveh^a, Susruta Samanta^a, Antonio De Nicola^{b,c}, Giuseppe Milano^{b,c} and
Danilo Roccatano^{a*}*

^a Jacobs University Bremen, Campus Ring 1, D-28759 Bremen, Germany

^b Dipartimento di Chimica e Biologia and NANOMATES, Research Centre for NANOMaterials and nanoTEchnology at Università di Salerno, I-84084 via Ponte don Melillo Fisciano (SA), Italy

^c IMAST Scarl-Technological District in Polymer and Composite Engineering, P.le Fermi 1, 80055 Portici (NA), Italy

AUTHOR EMAIL ADDRESS. d.roccatano@jacobs-university.de

CORRESPONDING AUTHOR FOOTNOTE.

*Dr. Giuseppe Milano. Dipartimento di Chimica e Biologia and NANOMATES, Research Centre for NANOMaterials and nanoTEchnology at Università di Salerno, I-84084 via Ponte don Melillo Fisciano (SA), Italy. Fax: +39 0899 65296, Tel: +39 089 969567, E-mail: gmilano@unisa.it

*Prof. Dr. Danilo Roccatano. Jacobs University Bremen, Campus Ring 1, D-28759, Bremen, Germany. Fax: +49 421 2003249, Tel: +49 421 2003144, E-mail: d.roccatano@jacobs-university.de.

ABSTRACT.

In this paper, we present a computational model of the adsorption and percolation mechanism of Poloxamers (Polyethylene Oxide (PEO) and Polypropylene Oxide (PPO) triblock copolymers) across a 1,2-dimyristoyl-*sn*-glycero-3-phosphocholine (DMPC) lipid bilayer. A particle-particle coarse-grained model was used to cope with the long timescale of the percolation process. The simulations have provided details of the interaction mechanism of Pluronics with lipid bilayer. In particular, the results have shown that polymer chains containing a PPO block with a length comparable to the DMPC bilayer thickness, such as P85, tends to percolate across the lipid bilayer. On the contrary, Pluronics with a shorter PPO chain, such as L64 and F38, insert partially into the membrane with the PPO block part while the PEO blocks remain in water on one side of the lipid bilayer. The percolation of the polymers into the lipid tail groups reduces the membrane thickness and increases the area per lipid. These effects are more evident for P85 than L64 or F38. Our findings are qualitatively in good agreement with published small angle X-ray scattering experiments that have evidenced a thinning effect of Pluronics on the lipid bilayer as well as the role of the length of the PPO block on the permeation process of the polymer through the lipid bilayer. Our theoretical results complement the experimental data with a detailed structural and dynamic model of Poloxamers at the interface and inside the lipid bilayer.

KEYWORDS. MARTINI coarse-grain model, membrane percolation, lipid bilayer, Pluronics, polymer simulations, interfacial phenomena.

INTRODUCTION.

Poloxamers (also known as their trademark name, Pluronics[®]) are amphiphilic linear ABA-type triblock copolymers with the B block composed of hydrophobic polypropylene oxide (PPO) and the two A blocks of hydrophilic polyethylene oxide (PEO) homopolymers. They have broad range of biomedical applications.¹⁻⁸ They are used, for example, as drug delivery systems,⁹⁻¹¹ in gene and cancer therapies.^{12,13} These broad ranges of applications are result of their peculiar properties in solutions and at biological interfaces. In particular, by changing the length of the polymer blocks, their solubility and other solution thermodynamic properties can be customized for specific applications.¹⁴

For drug delivery, hydrophobic drugs are embedded in block copolymer micelles to prevent their rapid turnover by increasing their biocompatibility and solubility. The drug release at cellular level involves molecular interaction mechanisms of the polymers with the membranes. The dynamics at atomic level of these processes is so far not easily accessible to experimental measurements and therefore many questions are still undisclosed on the molecular details of the interaction mechanisms.

Many experimental studies have been focused on the percolation capability of these polymers into lipid mono, and bilayer systems.¹⁵⁻²² From these studies, it is clear that the interaction of polymers with lipid layers is strongly influenced by the hydrophilic–lipophilic balance (HLB) caused by PEO/PPO block length ratio.²³ For instance, Pluronics with low HLB ratio (i.e. very large PPO block compared to the PEO blocks) can assist the permeation of small molecules through lipid bilayers,² show ionophoric activity,²⁴ act as chemo-sensitizing agents in cancer treatments,²⁵ and in some cases, they can even enter the cell.²³ On the other hand, Pluronics with large

1
2
3 HLB ratio (i.e. large PEO blocks), being too hydrophilic are unable to bind strongly
4
5 across cell membranes and their interaction is limited to the coating of the cellular
6
7 membrane surfaces.²³ Simple model membrane systems, such as, lipid Langmuir
8
9 monolayers, liposomes, giant unilamellar vesicles, and planar bilayers have been
10
11 investigated using different variety of techniques such as X-ray and neutron scattering
12
13 methods^{26,27} calorimetric measurements,^{19,28,29} fluorescence microscopy^{19,30,31} and
14
15 other microscopy techniques⁶ These studied have evidenced that the nature of the
16
17 interaction mainly depends on the length of PPO block compared to the bilayer
18
19 thickness. In fact, the PPO block has a stronger affinity to the hydrophobic tails of the
20
21 lipid bilayer than the PEO blocks that prefer to stay outside in contact with the
22
23 hydrophilic head-groups.^{9,32,33} Therefore, Pluronics with PPO block lengths less than
24
25 the thickness of the bilayer insert partially into the hydrophobic region of membrane
26
27 while those with PPO lengths comparable with the hydrophobic thickness of bilayer
28
29 can completely span across the membrane with their PEO blocks flanking in water in
30
31 the opposite sides of the bilayer.⁹ Unfortunately, these experimental evidences do not
32
33 provide the details of dynamics and molecular mechanism of these processes.³⁴ These
34
35 information can be easily obtained with molecular modeling, in particular with
36
37 molecular dynamics (MD) simulations. So far several computational studies have
38
39 been conducted on Pluronics at different levels of scale.³⁵⁻⁴⁰ However to the best of
40
41 our knowledge, none of these theoretical studies have addressed the interaction
42
43 mechanism of Pluronics with DMPC lipid bilayers. This lack of detailed atomistic
44
45 model of this process gave us the motivation for the study reported in this paper. We
46
47 have used MD simulations at Coarse-Grained (CG) level of scale to study the
48
49 interaction of Pluronic chains of different PEO and PPO block length with a DMPC
50
51 lipid bilayer. The use of CG MD simulations was necessary to cope with the time
52
53
54
55
56
57
58
59
60

1
2
3 scale of spontaneous diffusion of the polymers in the lipid bilayer that it goes beyond
4 the capability of ordinary full atomistic simulations. The MARTINI CG model was
5 adopted for this study to provide insights on the mechanism of this process. The
6 results of the study have been compared with the experimental SAXS data from
7 Firestone et al.^{9,33} The authors of these experimental papers proposed different
8 interaction models by comparing the periodicity of the diffraction peaks from a
9 DMPC-water-Pluronics mixture with the one from pure DMPC-water system. The
10 results of our simulations resulted in good agreement with these experimental data.
11
12
13
14
15
16
17
18
19

20
21 The paper is organized as follows: The details of the force field
22 parameterization for the CG model of the Pluronics are reported in the Supporting
23 Information (SI). The force field parameters for the Pluronics were validated by
24 calculating the radii of gyration (R_g) for PEO and PPO chains of different lengths in
25 water and comparing them with those from experimental measurements⁴¹ and
26 atomistic models.⁴² The Results and Discussions section is organized in two parts.
27
28 In the first part, the results of the Pluronics L64, P85 and F38 simulations in water
29 are reported. In the second part, simulations of three different Pluronics with the
30 DMPC lipid bilayer are presented. These simulations have been performed for
31 Pluronics- DMPC-water ternary mixtures and for Pluronics in water at the interface
32 of preformed DMPC lipid bilayer. Finally, in the Conclusions section, the main
33 results of this study are summarized.
34
35
36
37
38
39
40
41
42
43
44
45
46
47
48
49
50
51
52
53
54
55
56
57
58
59
60

METHODS.

Force-field parameterization.

The CG models used for MD simulations of polymers and lipids are based on the MARTINI force field.^{43,44} The model parameters for the polymers were optimized based on an atomistic model of the same polymers recently proposed by our group.^{42,45} The mapping scheme of the CG bead is the same as those adopted by similar CG model of PEO proposed by other groups.^{36,37} Each bead of the CG model for PEO and PPO includes three (C-O-C) and four (C(CH₃)-O-C) heavy atoms, respectively. Oxygen atoms were considered the centre of each bead for both polymers. From the atomistic simulations, the bond length and bond angle distributions were calculated considering the distance between oxygen atoms of two consecutive monomers and the angle formed by the two adjacent distance vectors as shown in Figure 1. Detailed information on CG force field parameterization and validation are available in the SI and the final optimized parameters are reported in Table 1.

As for the models proposed by Lee et al. (for PEO)³⁶ and Hatakeyama and Faller (for PEO and PPO)³⁹ we have also used the constant bead mass of 72 amu for efficiency reasons.^{39,43} Therefore, our model does not properly scale mass dependent properties because the real mass of PEO and PPO monomers are 44 and 58 amu, respectively. For these properties, only qualitative comparisons can be made with experimental data.

A comparison between non-bonded Lennard-Jones (LJ) parameters obtained by us and those reported by Lee et al.³⁶ for PEO show slight differences. But there are noticeable differences in the reference geometric parameters for bonds, bond-angles

1
2
3 and also absence of proper dihedrals in our model. The variations are probably due to
4
5 the different reference atomistic models used for the parameterization. Concerning the
6
7 PPO CG model, Hatakamaya and Faller³⁹ have proposed a MARTINI based model
8
9 for study of Pluronics. However, they did not follow the mapping procedure from
10
11 atomistic to CG model and bonded and non-bonded parameters of our PPO model are
12
13 completely different from their values. So far and to the best of our knowledge, other
14
15 models of the PPO based on MARTINI force field haven't been reported in literature..
16
17

18 19 **Simulation Setup.**

20
21 All MD simulations were performed using GROMACS (version 4.0.7) software
22
23 package.⁴⁶ A cut-off of 12 Å was applied for LJ and Coloumbic interactions. The LJ
24
25 potential was smoothly shifted to zero between 0.9 and 1.2 nm, and the Coulomb
26
27 potential was smoothly shifted to zero between 0.0 and 1.2 nm. The temperature and
28
29 pressure were maintained to the reference values (for the pressure, $P_0=1$ bar) using the
30
31 Berendsen thermostat and barostat⁴⁷ with coupling time constant of $\tau_T=0.3$ ps for
32
33 temperature and $\tau_P=3.0$ ps for the pressure. A time step of 30 fs was used. All errors
34
35 on the calculated properties have been evaluated using the block averaging method.⁴⁸
36
37
38

39
40 **Simulation of Pluronics.** Pluronics L64, P85 and F38 were chosen for the simulations
41
42 (see Table 2 for details). Each polymer was simulated at 293 K for ~900 ns in a
43
44 simulation box of ~9 nm/side containing ~7600 water molecules. The radius of gyration
45
46 of P85 was compared with the experimental value measured at the same temperature.⁴⁹
47
48

49
50 **Simulation of 1,2-dimethoxyethane (DME) and 1,2-dimethoxypropane (DMP)**
51
52 **with DMPC lipid bilayer.** Simulations of single DME/DMP inside the tail groups
53
54 and on top of lipid bilayer were performed at 310 K for 200 ns in a box of 10
55
56 nm/side containing ~7400 water molecules. Another set of simulation was
57
58
59
60

1
2
3 performed for nine molecules of each oligomer on top of the lipid bilayer for 400
4
5 ns at 310 K in a box of the same size. The bilayer used for both setups consisted of
6
7 300 phospholipid molecules.
8
9

10 **Simulations of Pluronics with DMPC bilayer.** Two sets of simulations have been
11
12 performed at 310 K. In the first set, the random conformation of one polymer chain was
13
14 solvated in a mixture of DMPC lipid/water; in the second set, the Pluronic chains were
15
16 positioned on the water phase on the top of an equilibrated DMPC lipid bilayer. The
17
18 details for two sets of simulations are as follows:
19
20

21 **a) Single chain.** One chain of each Pluronic L64, P85 and F38 was positioned in the
22
23 simulation box and then the DMPC lipid chains were randomly positioned in the box
24
25 while the remaining volume was filled with water molecules. In the second set, L64
26
27 and P85 Pluronic chains were positioned at a distance of 1-2 nm on the top of an
28
29 equilibrated DMPC lipid bilayer in water (see Table 3 for details).
30
31
32

33 **b) Multiple chains.** Five chains of Pluronic L64 and P85 were positioned randomly in
34
35 simulation boxes and then DMPC lipids were randomly positioned. For the Pluronics at
36
37 DMPC interface, the setup was repeated in the same way as for the single chain
38
39 simulation with five chains on top of the lipid bilayer (see Table 4 for details).
40
41
42

43 RESULTS AND DISCUSSION.

44
45 **Pluronics in Water.** Simulations were performed for three Pluronics, L64, P85 and F38
46
47 at 293 K. The R_g of the polymers are reported in Table 5. R_g of P85 unimer at dilute
48
49 conditions was available from recent small-angle neutron scattering (SANS)
50
51 measurements.⁴⁹ The value of $R_g = 2.19 \pm 0.04$ nm, obtained from the simulation is in
52
53 good agreement with the experimental value of $\sim 1.95 \pm 0.2$ nm at 293K.⁴⁹ Pluronic F38
54
55 has a considerably bigger R_g than the one for P85 because of longer PEO blocks. L64
56
57
58
59
60

1
2
3 has the smallest value due to short PEO blocks. R_g values of PPO blocks were also
4
5 calculated (Table 5). P85 shows the largest value of 1.15 nm for PPO block. This value
6
7 is comparable to the thickness (1.65 nm) of the hydrophobic part of lipid bilayer. For
8
9 F38 and L64, the R_g values of the PPO blocks (0.82 nm and 1.03 nm, respectively) are
10
11 both shorter than the bilayer leaflet, especially for F38. Therefore, from these values,
12
13 we expect (as the experimental results also suggests)⁹ that P85 can span its PPO block
14
15 through the lipid bilayer while for L64 and F38 it is less likely to happen.
16
17

18
19 **DME and DMP with DMPC bilayer.** These simulations were used to test the CG
20
21 force field against atomistic simulations of the same system. Therefore, we
22
23 simulated DME and DMP with DMPC lipid bilayer in the same conditions as
24
25 reported in our previous study.⁵⁰
26
27

28
29 Starting with simulation of one DME/DMP inside tail groups and on top of
30
31 the bilayer, we calculated the density profiles for both molecules (shown in Figure
32
33 2) at different simulation times of 5, 50, and 200 ns. For simulations starting with
34
35 single DME/DMP molecule located inside the tail groups, the density profiles at 5
36
37 ns (equivalent to 50 ns of atomistic simulation) follow the same trend as the
38
39 atomistic simulations.⁵⁰ The DME molecule was mostly localized in the head
40
41 group region and less in the water region, while DMP prefers to remain in the tail
42
43 group region. After 50 ns of CG simulation, the density profiles remain similar to
44
45 those at 5 ns. However, after 200 ns, the DMP density profile shows the presence
46
47 of the molecule also outside the bilayer in the water region. This shows that DMP
48
49 molecule can diffuse in water in a time range of hundred to microsecond. This
50
51 behaviour stems from the fact that DMP, as shortest oligomer of PPO is still
52
53 soluble in water.⁴⁵
54
55
56

57
58 We also tested the density profiles for the DME/DMP molecules localized
59
60

1
2
3 in the water phase on the top of the lipid bilayer. Again the results are consistent
4
5 with the atomistic simulations within 5 ns of simulations as shown in Figure 2.
6
7 After 50 and 200 ns DME and DMP density show their better localization in the
8
9 head and tail groups, respectively.
10

11
12 The effect of the concentration was tested by simulations of nine DME or
13
14 DMP molecules on top of bilayer. Figure 3 is showing the snapshots of the
15
16 simulations at 0 ns and after 400 ns. The density profiles presented in Figure 4
17
18 were calculated for 5, 50, 200 and 400 ns. Consistently with atomistic simulations,
19
20 after 5 ns, a partial penetration of DMEs and DMPs into lipid bilayer head and tail
21
22 groups, respectively, was observed. The density profiles become more pronounced
23
24 after 50 ns in these two lipid regions. After 200 ns, a complete localization of the
25
26 molecules in head groups for DME and in tail regions for DMP was observed.
27
28

29
30 Finally, for the DME and DMP oligomers, we have compared potential mean
31
32 force (PMF) profiles of permeation through the lipid bilayer, using umbrella sampling
33
34 from atomistic simulations,⁵⁰ with those obtained in the same manner from CG
35
36 simulations. The results of this comparison show as expected a fair agreement for the
37
38 DME but a larger difference for the DMP (see Figure6S in SI). In our CG model DMP
39
40 has a stronger relative affinity for the lipid part due to the Lennard-Jones interaction
41
42 energy with the lipid tail beads. Attempts to improve the relative agreement between
43
44 the atomistic and the CG for DMP by changing the interaction parameters with the
45
46 lipid bilayer resulted in a reduced interaction tendency of PPO block of Pluronics
47
48 chain with the tail region of the lipid bilayer (data not reported). This behavior was in
49
50 contradiction with the results of our atomistic simulations and with the experimental
51
52 data; therefore we resolved to use the original parameters. It is likely that the
53
54 approximate model of DMP does not account the entropic difference with the DME
55
56
57
58
59
60

1
2
3 due to its different structure. The change of the enthalpic term alone cannot account of
4
5 the correct thermodynamics of the percolation process. On the other hand, the
6
7 difference observed between the atomistic and CG model PMF curve are of the order
8
9 of ~ 15 kJ/mol, which is in the same order of magnitude observed in the comparison of
10
11 atomistic PMF versus the MARTINI CG one for the extraction of single lipid from the
12
13 bilayer (see Figure 5 in Ref. 44).
14
15

16 17 18 19 **Random ternary mixture of polymers, phospholipids and water molecules.**

20
21 **Simulation of single Pluronic chain.** In this part of the study, we have simulated a
22
23 single chain of Pluronics L64, P85 and F38 in ternary mixtures (details are reported in
24
25 the Methods section). According to the experimental work of Firestone et al.,⁴ the PPO
26
27 and PEO length affects the interaction of polymers with DMPC lipid bilayer. From their
28
29 SAXS results, they suggested two possible interactions between Pluronic and bilayer,
30
31 which mainly depend on the PPO block length. In the case of PPO block length less
32
33 than the bilayer hydrophobic length, their experimental data suggested a partial
34
35 insertion of PPO block in the lipid bilayer. In the other case, when the length is
36
37 comparable or longer than of bilayer hydrophobic length, a complete insertion and
38
39 spanning of PPO block across bilayer occurs by leaving the PEO blocks in water and on
40
41 the two opposite sides of the membrane.
42
43
44
45

46
47 To verify these two scenarios with molecular models, we have considered
48
49 Pluronics with different PPO block lengths such as F38, L64 and P85 and have
50
51 performed simulations for 500 ns in each case. The Pluronic F38 has the shortest PPO
52
53 block of 15 monomers, P85 has the longest one of 40 monomers, and L64 has the PPO
54
55 block length of 30 monomers. Figure 5 shows snapshots from simulations of one
56
57
58
59
60

1
2
3 polymer chain in lipid-water mixtures at 310 K right after the formation of the lipid
4
5 bilayers and the equilibration of the polymer in the two-phase system.
6
7

8 The lipid bilayer formation is quite fast and it occurs in ~10 to 20 ns depending
9
10 on the length of the Pluronic. The simulation results suggest that PPO block is the
11
12 dominant factor in interaction and insertion of Pluronic in the membrane. As we
13
14 expected from R_g values of PPO blocks in water, L64 and F38 polymers show a partial
15
16 insertion because of their shorter PPO blocks. On the contrary, the P85 has a PPO block
17
18 long enough to cross the membrane thickness (as shown in the snapshot of Figure 5).
19
20 Although the formation of the bilayer occurs quite fast, the polymer localization takes
21
22 longer time after the bilayer is formed. The polymer equilibration time depends on the
23
24 PEO and PPO length. For instance, for P85, even after the lipid bilayer is formed, the
25
26 two PEO blocks are still in tail groups and gradually get repelled outside in the water
27
28 phase on the opposite sides of membrane. The PPO block remains completely inside as
29
30 shown in last picture of Figure 6. This behavior was also reported in our previous
31
32 atomistic study of DME and DMP interaction with DMPC lipid bilayer.⁵¹
33
34
35
36

37 For other Pluronic like the F38, since PPO block is shorter than the bilayer
38
39 leaflet, it cannot extend completely and reach the other side of bilayer. Therefore, as
40
41 both PEO blocks are repelled outside the lipid bilayer, they pull the PPO block to the
42
43 same direction, in this way, the PPO block remains inside the lipid bilayer adopting a U
44
45 shaped configuration (see Figure 5). All these results fully support the hypothesis
46
47 suggested by Firestone et al.^{9,33} based on their experimental results, on the possible
48
49 modus of interaction of Pluronics with the DMPC lipid bilayer (see Figure 1 from the
50
51 work of Firestone et al.).⁹
52
53
54

55 To evaluate these interactions more quantitatively, we have calculated the
56
57 electron density for polymers and phosphate groups plus water as shown in Figure 7.
58
59
60

1
2
3 The bilayer thickness, d_B , with and without the presence of Pluronics, was calculated
4 from electron density profiles using phosphates peak-to-peak distances. The value of d_B
5 without Pluronics was 4.01 nm, whereas in the presence of L64, P85 and F38 the
6 distances were reduced to 3.40, 3.21, 3.43 nm (errors are less than 0.01 nm),
7 respectively (Figure 7 a). The decrease of the d_B values clearly indicates a bilayer
8 thinning effect due to the presence of the polymers. The thinning effect was also
9 observed from Lee and Firestone experimental results.³³ In addition, the electron
10 density in water (Figure 7b) is also qualitatively comparable to the experimental results
11 for different PEO lengths.³³ This part is mainly a region of localization of PEO into
12 water region. In this region, P85 shows a peak at ~ 3.25 nm and proves more PEO
13 localization on the surface of bilayer. This is while F38 is showing broader feature and
14 in case of L64 there is no pronounced peak.

15
16
17
18
19
20
21
22
23
24
25
26
27
28
29
30 The area per lipid was calculated for the bilayer with and without the polymers.
31
32 The value of area per lipid for pure bilayer resulted in 0.62 nm^2 . However, the value
33 increased to 0.66 nm^2 for P85 and 0.64 nm^2 for both L64 and F38 (Figure 4S in SI).
34
35 The errors in all case are smaller than 0.01 nm^2 . The slightly increase of the area per
36 lipid is consistent with the thinning effect

37
38
39
40
41 **Simulations of Multiple Pluronic chains.** To test the effect of the Pluronic
42 concentration on the lipid bilayer, 5 chains of Pluronics L64 and P85, respectively, were
43 simulated with random lipids and on the top of the DMPC lipid bilayer.
44
45
46
47

48
49 Figure 8 shows the configuration of the systems after ~ 500 ns of simulation.
50
51 The formation of lipid bilayer took only ~ 20 ns. As shown in the figure, some P85
52 chains did not completely extend through the bilayer. For both Pluronics, the PPO
53 blocks of the different chains inside the bilayer tend to aggregate.
54
55
56
57
58
59
60

1
2
3 In Figure 9, the calculated electron density for phosphate head groups, Pluronic
4 and water are shown. The average bilayer thicknesses were 3.10 nm and 3.02 nm
5 (errors are less than 0.01) for L64 and P85, respectively. These values are 9-6% smaller
6 than those for single chain simulations, evidencing a concentration dependence of the
7 bilayer thinning effect. In the water region (Figure 9b), the P85 density drops down
8 moving away from bilayer surface while, for L64, the density shows a broader
9 distribution. The calculated area per lipid increased up to 0.66 ± 0.01 nm² and 0.71 ± 0.01
10 nm² for bilayer with L64 and P85, respectively (Figure 4S in SI). These values suggest
11 that area per lipid increases with the length of the polymer.
12
13
14
15
16
17
18
19
20
21
22

23 **Polymer on the top of a pre-formed DMPC lipid bilayer.**

24
25
26 **Simulation of single Pluronic chain.** In this part, the results of the simulations of P85
27 and L64 Pluronic chains with a pre-formed DMPC bilayer are reported. The aim of
28 these sets of simulations was to understand the process and spontaneous diffusion of the
29 polymer through the bilayer within the timescale of our simulations. The polymers were
30 positioned in the water phase ~1-2 nm away from the bilayer surface and then
31 simulated for 900 ns. Figure 10 shows snapshots from different stages of the simulation
32 of P85 with DMPC bilayer (the results for L64 are shown in Figure 5S in SI). The
33 figure shows that the adsorption of the PEO block in the membrane surface is the first
34 stage for the polymer interaction. The second stage is characterized by the percolation
35 of the PPO block through the head groups of the lipid bilayer. The second process is
36 quite fast and it occurs in about 2 ns. This process starts with PPO block getting in
37 contact with the surface of bilayer (Figure 10). However, it takes 227.5 ns for PPO to
38 get close to surface area of the bilayer. Hence, the polymer penetrates in less than 1 ns
39 into the bilayer head-group region and comes in contact with the hydrophobic lipid
40 tails. From this point, the insertion of the whole chain occurs in ~1 ns. Once the PPO
41
42
43
44
45
46
47
48
49
50
51
52
53
54
55
56
57
58
59
60

1
2
3 block is completely inside the lipid bilayer (533.0 ns), it remains there for the rest of the
4
5 simulation (~400 ns more), whereas PEO block remains on the bilayer surface.
6
7

8 In Figure 11, the density profiles for L64 (entering from the left side of the
9 bilayer) and P85 (entering from the right side of the bilayer) before and after the
10 insertion of PPO in the lipid bilayer are reported. The density profiles indicate that PEO
11 mainly remains in the head group region while PPO penetrates in the tail group region
12 of the bilayer. The penetration of PPO in tail groups is more extended for P85 than L64
13 because of longer PPO block. For both cases, PPO densities near head-groups are very
14 low. This is due to the fast insertion of the PPO block from the water phase to the
15 bilayer inner part. As shown in the Figure 11, after PPO inserts the tails, it becomes less
16 compact. In Table 6, the average values of R_g of Pluronic PPO blocks, inside and
17 outside the lipid bilayer, are reported. In Figure 12, the time series of the same R_g are
18 also shown. Dashed lines indicate the times at which PPO block is completely inside
19 the bilayer. The dashed lines for L64 and P85 are located at 86 ns and 219 ns,
20 respectively. From Table 6 and Figure 12, it is evident that PPO R_g increases when
21 polymers insert into the bilayer.
22
23
24
25
26
27
28
29
30
31
32
33
34
35
36
37
38

39 In these simulations, only the partial interaction of the Pluronic with lipid
40 bilayer was observed. For P85, despite the long PPO block, a complete insertion of the
41 block, even after the extension of the simulation up to ~2 μ s, was not observed. This
42 was due to the high hydrophobic barrier for the hydrophilic PEO, which in the
43 simulation conditions cannot be overcome. Experimental studies have shown that other
44 mechanisms may be involved with the interaction of the Pluronic with biological
45 membrane that can help the translocation of PEO block from one side to the other of
46 the lipid bilayer.^{24,52} One proposed mechanism involved is an increase in the flip-flop
47 movement of individual lipid molecules upon the interaction of Pluronic with the head
48
49
50
51
52
53
54
55
56
57
58
59
60

1
2
3 groups.²⁴ Since these processes are supposed to occur at very slow rate (average
4
5 lifetime from several hours to several days)^{53,54} then they could not be observed in our
6
7 simulations.

8
9
10 **Simulations of multiple Pluronic chains.** In Figure 13, snapshots from the
11
12 simulations show the interactions of five L64 and P85 Pluronic chains with a DMPC
13
14 bilayer. At the beginning of the simulations, formation of aggregates was observed for
15
16 both L64 and P85 chains. The aggregation involved the formation of a PPO core that
17
18 remained exposed to the water phase while the PEO parts coated the bilayer surface as
19
20 shown in the Figure 13. This process delayed the insertion of individual chains into the
21
22 lipid bilayer and, after 900 ns, only two L64 chains were able to insert their PPO blocks
23
24 inside the membrane and the other two L64 chains inserted only after 1.7 μ s. For P85
25
26 chains, even after 1.7 μ s no insertion was observed (Figure 13, at 1.7 μ s).

27
28
29
30
31 Comparing the two simulations, it seems that the length of PEO is an important
32
33 factor in the way Pluronics interact with the lipid bilayer, especially when the polymer
34
35 concentration increases. In particular, the PPO entanglement also seems to play a role
36
37 in percolation rate. To check whether this delay is due to the PEO surface coating or the
38
39 PPO entanglement, further simulations were performed with four PEO chains (with
40
41 same length of Pluronics L64 and P85) and only one Pluronic chain. In Figure 14, the
42
43 system A is including PEO chains and P85 while system B is containing PEO chains and
44
45 L64. System A contains around 1.6 times more PEO chains than B. In this way, we
46
47 could figure out the role of PEO surface coating without the effect of PPO
48
49 entanglement. The results of the simulation showed that the PPO block of Pluronic L64
50
51 could penetrate into the lipid bilayer in \sim 85 ns, which is very close to the first passage
52
53 time observed from the simulation of the single L64 chain (see Figure 5S in SI).
54
55 However, for the P85 the insertion occurred around 1 μ s, which is \sim 4 time longer than
56
57
58
59
60

1
2
3 for the time required for the isolated chain (229.4 ns, see also Figure 10). From these
4
5 simulations, it seems clear that both PPO entanglement and PEO surface coating play a
6
7 role in the rate of permeation of the polymer into the lipid bilayer. In fact, the relative
8
9 higher concentration of the PEO blocks and the PPO aggregation can both prevent the
10
11 contact of PPO blocks with the bilayer surface and, therefore, reduce the insertion rate.
12
13 This interesting finding about effect of PEO coating is supporting the experimental
14
15 fluorescent microscopy measurements³¹ that show the absence of diffusion through
16
17 cellular membrane for Pluronics with long PEO blocks. Our simulations have also
18
19 showed; however the PPO entanglements may play a role in this process.
20
21
22
23
24
25

26 **CONCLUSIONS.**

27
28 This work was aimed to understand the interaction of Poloxamers at the molecular level
29
30 with lipid bilayer using coarse-grained simulations based on the MARTINI force field.
31
32 The CG model for Pluronics was parameterized using simulation data of previously
33
34 reported atomistic model.^{42,45} The CG models of PEO, PPO and Pluronics show good
35
36 agreement with the atomistic simulation data as well as with the experimentally
37
38 determined properties of these polymers in water (i.e., radius of gyration).
39
40
41
42

43 We have modeled and studied the interaction of Pluronics with DMPC lipid
44
45 bilayer. The results of the study are consistent with experimental SAXS data and
46
47 provide molecular details of the interaction. First, the role of PPO block length was
48
49 shown as a critical determinant of the mode of insertion of the copolymer in the lipid
50
51 bilayer. A poor permeation of the polymer was observed for PPO block lengths less
52
53 than the bilayer leaflet while allowing the PEO chains to extend on the top of the lipid
54
55 bilayer. On the contrary, when the PPO block has a length comparable to the bilayer
56
57
58
59
60

1
2
3 thickness, it can span across the lipid bilayer with the PEO blocks flanking on the
4
5 opposite sides of bilayer in the water phase. Second, the calculated electron density
6
7 profiles evidence a thinning effect of Pluronics on the bilayer, which is consistent with
8
9 the experimental SAXS data. This effect is followed by an increase in the area per lipid.
10
11 Our results indicate that DMPC lipid bilayer in the presence of the Pluronics L64 or
12
13 P85 Pluronics tends to be more permeable with a more evident effect for the P85.
14
15

16
17 Simulations of Pluronics on top of the lipid bilayer were used to reproduce the
18
19 actual phenomenon of interaction of polymer with biological membranes. The results of
20
21 these simulations indicates that the process mainly proceed by a two-stage mechanism.
22
23 First, the PEO get adsorbed on the hydrophilic surface of the membrane. This makes
24
25 the PPO block to get close to the bilayer surface. Second, while the PEO remains close
26
27 to the head groups of the lipid bilayer, the PPO starts penetrating inside the tail regions.
28
29 Interestingly, as the polymer concentration increases, the rate of diffusion of the
30
31 polymer in the bilayer tail region slows down. Our simulations indicate that this effect
32
33 can be caused due to both the PEO concentration and the PPO block aggregation that
34
35 delays, and in case of longer chains, prevent the contact of PPO blocks with the bilayer
36
37 surface, thus reducing the chance of their insertion. This finding is consistent with the
38
39 experimental studies³¹ showing the interactions of Pluronics with long PEO blocks are
40
41 only limited to the covering of the membrane surfaces.
42
43
44
45
46
47
48

49 **ACKNOWLEDGEMENT.**

50
51 This project is funded by the Deutsche Forschungsgemeinschaft (DFG) for the
52
53 project titled “The Study of Detailed Mechanism of Polymers/Biological
54
55 Membrane Interactions Using Computer Simulation” (RO 3571/3-1).
56
57
58
59
60

SUPPORTING INFORMATION.

The details of MARTINI CG force field parameterization & validation and figure for interaction of Pluronic L64 with DMPC bilayer are available in the Supporting Information. This material is available free of charge via the Internet at <http://pubs.acs.org>.

REFERENCES.

- (1) Xin, X.; Xu, G. Y.; Zhang, Z. Q.; Chen, Y. J.; Wang, F. *Eur. Polym. J.* **2007**, *43*, 3106.
- (2) Chiappetta, D. A.; Sosnik, A. *Eur. J. Pharm. Biopharm.* **2007**, *66*, 303.
- (3) Escobar-Chavez, J. J.; Lopez-Cervantes, M.; Naik, A.; Kalia, Y. N.; Quintanar-Guerrero, D.; Ganem-Quintanar, A. *J. Pharm. Pharmaceut. Sci.* **2006**, *9*, 339.
- (4) Kabanov, A. V.; Batrakova, E. V.; Alakhov, V. Y. *Adv. Drug Delivery Rev.* **2002**, *54*, 759.
- (5) Wasungu, L.; Marty, A. L.; Bureau, M. F.; Kichler, A.; Bessodes, M.; Teissie, J.; Scherman, D.; Rols, M. P.; Mignet, N. *J. Controlled Release* **2011**, *149*, 117.
- (6) Fusco, S.; Borzacchiello, A.; Netti, P. A. *J. Bioact. Compat. Polym.* **2006**, *21*, 149.
- (7) Erukova, V. Y.; Krylova, O. O.; Antonenko, Y. N.; Melik-Nubarov, N. *S. Biochim. Biophys. Acta, Biomembr.* **2000**, *1468*, 73.
- (8) Frey, S. L.; Zhang, D. S.; Carignano, M. A.; Szleifer, I.; Lee, K. Y. C. *J. Chem. Phys.* **2007**, *127*.
- (9) Firestone, M. A.; Wolf, A. C.; Seifert, S. *Biomacromolecules* **2003**, *4*, 1539.
- (10) Maskarinec, S. A.; Wu, G. H.; Lee, K. Y. C. *Cell Injury: Mechanisms, Responses, and Repair* **2005**, *1066*, 310.
- (11) Amado, E.; Blume, A.; Kressler, J. *React. Funct. Polym.* **2009**, *69*, 450.
- (12) Amado, E.; Kressler, J. *Curr. Opin. Colloid Interface Sci.* **2011**, *16*, 491.
- (13) Peetla, C.; Stine, A.; Labhassetwar, V. *Mol. Pharmaceutics* **2009**, *6*, 1264.
- (14) Carlsson, M.; Hallen, D.; Linse, P. *J. Chem. Soc.-Faraday Trans.* **1995**, *91*, 2081.
- (15) Amado, E.; Kerth, A.; Blume, A.; Kressler, J. *Langmuir* **2008**, *24*, 10041.

- 1
2
3 (16) Hussain, H.; Kerth, A.; Blume, A.; Kressler, J. *J. Phys. Chem. B* **2004**,
4 *108*, 9962.
5 (17) Frey, S. L.; Lee, K. Y. C. *Langmuir* **2007**, *23*, 2631.
6 (18) Feitosa, E.; Winnik, F. M. *Langmuir* **2010**, *26*, 17852.
7 (19) Chieng, Y. Y.; Chen, S. B. *J. Phys. Chem. B* **2009**, *113*, 14934.
8 (20) Wu, G. H.; Khant, H. A.; Chiu, W.; Lee, K. Y. C. *Soft Matter* **2009**, *5*,
9 1496.
10 (21) Schulz, M.; Olubummo, A.; Binder, W. H. *Soft Matter* **2012**, *8*, 4849.
11 (22) Binder, W. H. *Angew. Chem. Int. Ed.* **2008**, *47*, 3092.
12 (23) Kabanov, A. V.; Batrakova, E. V.; Miller, D. W. *Adv. Drug Delivery*
13 *Rev.* **2003**, *55*, 151.
14 (24) Krylova, O. O.; Pohl, P. *Biochemistry* **2004**, *43*, 3696.
15 (25) Miller, D. W.; Batrakova, E. V.; Kabanov, A. V. *Pharm. Res.* **1999**, *16*,
16 396.
17 (26) Wu, G. H.; Majewski, J.; Ege, C.; Kjaer, K.; Weygand, M. J.; Lee, K.
18 *Y. C. Biophys. J.* **2005**, *89*, 3159.
19 (27) Majewski, J.; Kuhl, T. L.; Wong, J. Y.; Smith, G. S. *Rev. Mol.*
20 *Biotechnol.* **2000**, *74*, 207.
21 (28) Castile, J. D.; Taylor, K. M. G.; Buckton, G. *Int. J. Pharm.* **2001**, *221*,
22 197.
23 (29) Heerklotz, H.; Seelig, J. *Biochim. Biophys. Acta, Biomembr.* **2000**,
24 *1508*, 69.
25 (30) Pembouong, G.; Morellet, N.; Kral, T.; Hof, M.; Scherman, D.;
26 Bureau, M. F.; Mignet, N. *J. Controlled Release* **2011**, *151*, 57.
27 (31) Maskarinec, S. A.; Hannig, J.; Lee, R. C.; Lee, K. Y. C. *Biophys. J.*
28 **2002**, *82*, 1453.
29 (32) Firestone, M. A.; Seifert, S. *Biomacromolecules* **2005**, *6*, 2678.
30 (33) Lee, B.; Firestone, M. A. *Biomacromolecules* **2008**, *9*, 1541.
31 (34) Wang, J. Y.; Chin, J. M.; Marks, J. D.; Lee, K. Y. C. *Langmuir* **2010**,
32 *26*, 12953.
33 (35) Wang, Q. F.; Keffer, D. J.; Nicholson, D. M. *J. Chem. Phys.* **2011**, *135*.
34 (36) Lee, H.; de Vries, A. H.; Marrink, S. J.; Pastor, R. W. *J. Phys. Chem. B*
35 **2009**, *113*, 13186.
36 (37) Bedrov, D.; Ayyagari, C.; Smith, G. D. *J. Chem. Theory Comput.* **2006**,
37 *2*, 598.
38 (38) Fischer, J.; Paschek, D.; Geiger, A.; Sadowski, G. *J. Phys. Chem. B*
39 **2008**, *112*, 13561.
40 (39) Hatakeyama, M.; Faller, R. *Phys. Chem. Chem. Phys.* **2007**, *9*, 4662.
41 (40) Nawaz, S.; Redhead, M.; Mantovani, G.; Alexander, C.; Bosquillon,
42 C.; Carbone, P. *Soft Matter* **2012**, *8*, 2744.
43 (41) Kawaguchi, S.; Imai, G.; Suzuki, J.; Miyahara, A.; Kitano, T. *Polymer*
44 **1997**, *38*, 2885.
45 (42) Stubbs, J. M.; Potoff, J. J.; Siepmann, J. I. *J. Phys. Chem. B* **2004**, *108*,
46 17596.
47 (43) Marrink, S. J.; de Vries, A. H.; Mark, A. E. *J. Phys. Chem. B* **2004**,
48 *108*, 750.
49 (44) Marrink, S. J.; Risselada, H. J.; Yefimov, S.; Tieleman, D. P.; de Vries,
50 A. H. *J. Phys. Chem. B* **2007**, *111*, 7812.
51 (45) Hezaveh, S.; Samanta, S.; Milano, G.; Roccatano, D. *J. Chem. Phys.*
52 **2011**, *135*.
53
54
55
56
57
58
59
60

- 1
2
3 (46) Hess, B.; Kutzner, C.; van der Spoel, D.; Lindahl, E. *J. Chem. Theory*
4 *Comput.* **2008**, *4*, 435.
5 (47) Berendsen, H. J. C.; Postma, J. P. M.; Vangunsteren, W. F.; Dinola, A.;
6 Haak, J. R. *J. Chem. Phys.* **1984**, *81*, 3684.
7 (48) Flyvbjerg, H.; Petersen, H. G. *J. Chem. Phys.* **1989**, *91*, 461.
8 (49) Hammouda, B. *Eur. Polym. J.* **2010**, *46*, 2275.
9 (50) Samanta, S.; Hezaveh, S.; Milano, G.; Roccatano, D. *J. Phys. Chem. B*
10 **2012**, *116*, 5141.
11 (51) Hager, S. L.; Macrury, T. B. *J. Appl. Polym. Sci.* **1980**, *25*, 1559.
12 (52) Yaroslavov, A. A.; Melik-Nubarov, N. S.; Menger, F. M. *Acc. Chem.*
13 *Res.* **2006**, *39*, 702.
14 (53) Kornberg, R. D.; Mcconnel.Hm. *Biochemistry* **1971**, *10*, 1111.
15 (54) Wimley, W. C.; Thompson, T. E. *Biochemistry* **1990**, *29*, 1296.
16
17
18
19
20
21
22
23
24
25
26
27
28
29
30
31
32
33
34
35
36
37
38
39
40
41
42
43
44
45
46
47
48
49
50
51
52
53
54
55
56
57
58
59
60

TABLES:

Table 1. CG force field parameters for bonded and non-bonded interactions used in this work to model PEO and PPO polymers.

PEO bonded parameters			
Bond		Angle	
b(nm)	K (kJ mol ⁻¹ nm ⁻²)	θ(deg)	K (kJ mol ⁻¹)
0.28	8000	155	40
PEO Non-bonded parameters			
		σ (nm)	ε (kJ mol ⁻¹)
PEO-PEO		0.48	3.5
PEO-W		0.47	4.5
PPO bonded parameters			
Bond		Angle	
b(nm)	K (kJ mol ⁻¹ nm ⁻²)	θ(deg)	K (kJ mol ⁻¹)
0.28	5000	140	40
PPO Non-bonded parameters			
		σ (nm)	ε (kJ mol ⁻¹)
PPO-PPO		0.50	2.6
PPO-W		0.47	3.5
Other Non-bonded parameter			
		σ (nm)	ε (kJ mol ⁻¹)
PEO-PPO		0.47	2.9
W-W		0.47	5.0

Table 2. Description of the Pluronics block lengths used in this study.

	N. PEO block	N. PPO block
P85	26	40
L64	13	30
F38	43	15

Table 3. Summarized information of the systems simulated for single chain of Pluronic in random mixture and on the top of bilayer surface.

Single chain	Ternary mixture			Bilayer		
	Box size (nm)	Waters	Lipids	Box size (nm)	Waters	Lipids
P85	8.5	5540	300	10	7400	300
L64	8.5	5540	300	10	7400	300
F38	8.5	5540	300			

Table 4. Summarized information of the systems simulated for multi-chains of Pluronic in random mixture and on the top of bilayer surface.

Polymer	Ternary mixture			Bilayer		
	Box size (nm)	Water	Lipids	Box size (nm)	Water	Lipids
P85	9.5	6400	310	10	7379	287
L64	9.5	6400	310	10	7379	287

Table 5. Radius of gyration values for Pluronic in water at 293 K.

R_g	L64 (nm)	P85 (nm)	F38 (nm)
Pluronic	1.68±0.08	2.19±0.20	3.25±0.22
PPO	1.03±0.10	1.15±0.31	0.82±0.01

Table 6. Radius of gyration values for PPO blocks inside and outside bilayer at 310 K.

	P85 (nm)	L64 (nm)
Outside bilayer	0.96±0.04	0.93±0.03
Inside bilayer	1.59±0.12	1.30±0.03

FIGURES:

Figure 1. PEO (left) and PPO (right) mapping scheme from atomistic to CG MARTINI model.

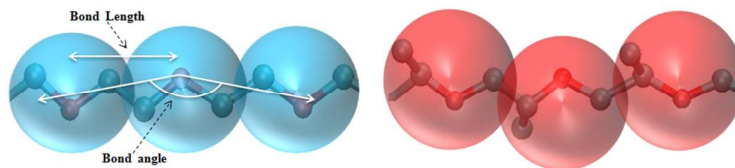
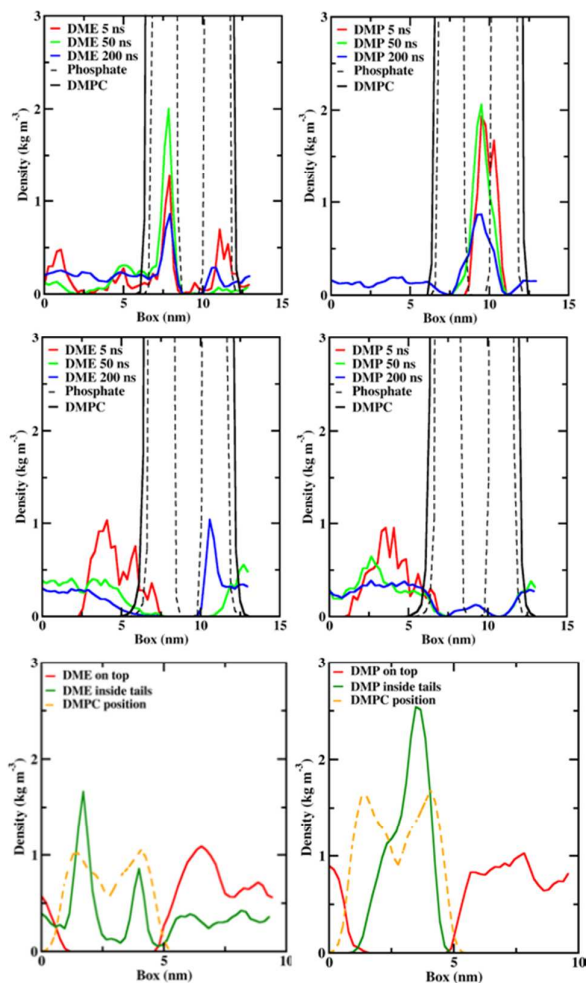


Figure 2. Density profiles for single DME (first column) and DMP (second column).

The profiles for DME/DMP in the lipid tails region (top row) and those for the same molecules on top of DMPC bilayer (middle row) at 310 K are shown. The results for atomistic simulations⁵⁰ are reported in the last row for comparison.



1
2
3 **Figure 3.** Snapshots of simulations of nine DME/DMP on top of DMPC bilayer at 0 ns
4 (top row) and 400 ns (bottom row). White points are water molecules. The bilayer tail
5 (top row) and 400 ns (bottom row). White points are water molecules. The bilayer tail
6 and head group regions are within the range indicated with arrows. DMEs/DMPs are
7 shown in blue and red, respectively.
8
9
10
11
12
13
14
15
16
17
18
19
20
21
22
23
24
25
26
27
28
29
30
31
32
33
34
35
36
37
38
39
40
41
42
43
44
45
46
47
48
49
50
51
52
53
54
55
56
57
58
59
60

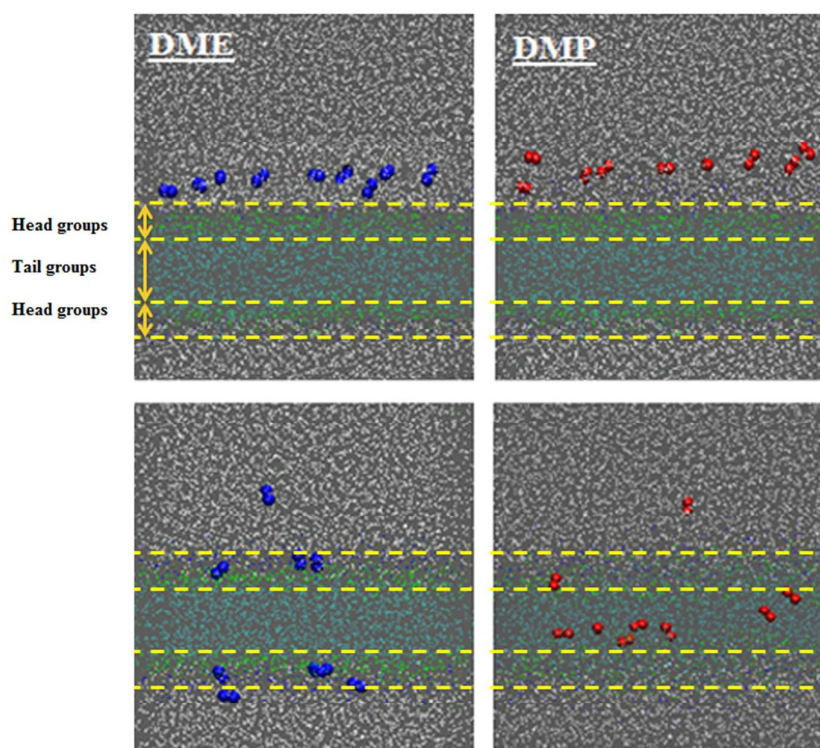


Figure 4. Density profiles for nine DME/DMP molecules on the top of DMPC bilayer at 310 K.

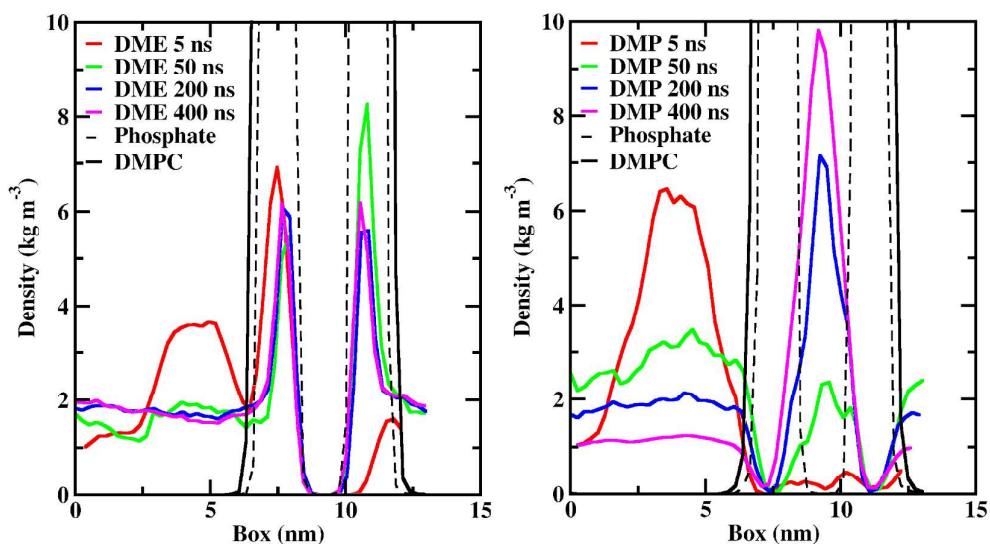


Figure 5. Interactions of Pluronics (different PPO block lengths) with DMPC bilayer at 310 K. The snapshots were taken right after bilayer formation. Numbers in parenthesis are showing the time needed for the bilayer formation. For clarity, water molecules are not shown.

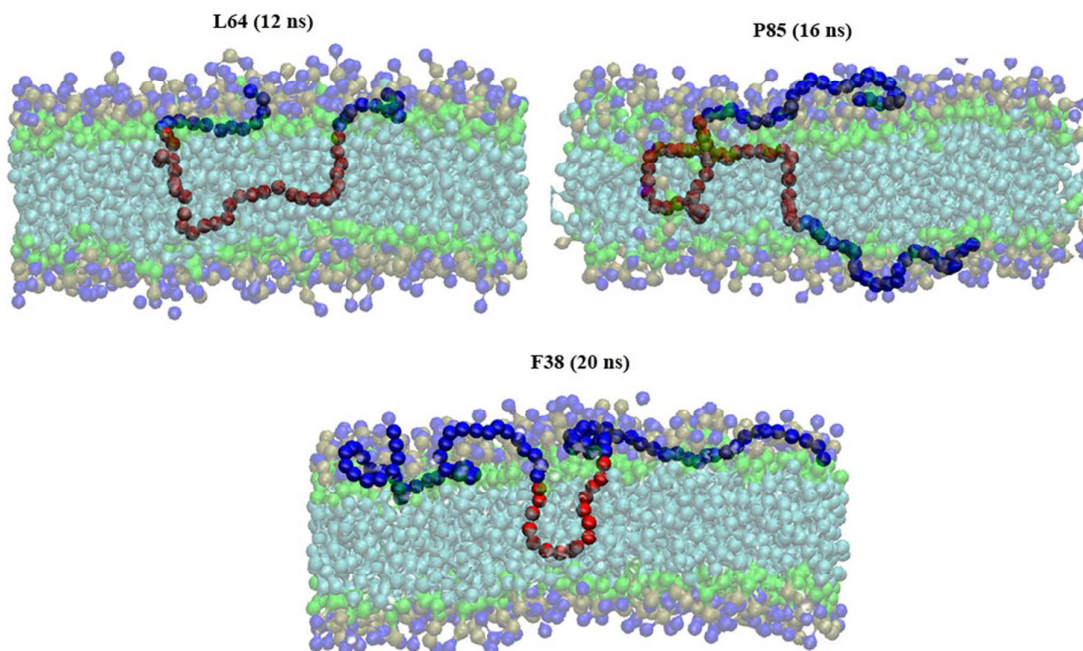


Figure 6. Snapshots of timeframes along the simulation of P85 in a random mixture of water and lipid. For clarity, water molecules are not shown.

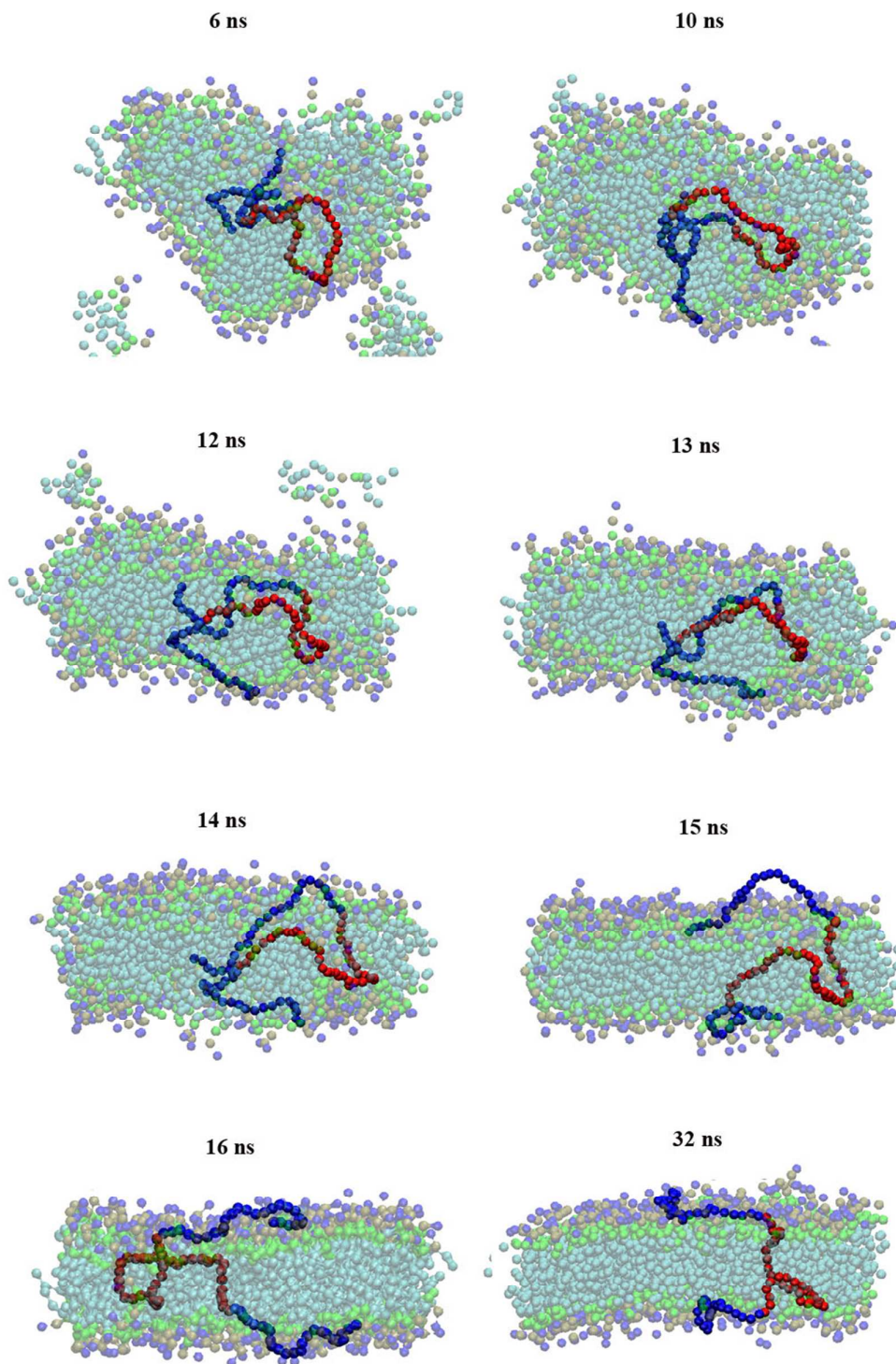


Figure 7. Electronic density profile for DMPC bilayer with Pluronics. The dashed line is showing electron density of phosphate groups and water. The total density range is from -4.5 to +4.5 that for clarity is divided into two parts, one for the membrane region (top) and one for water region (bottom).

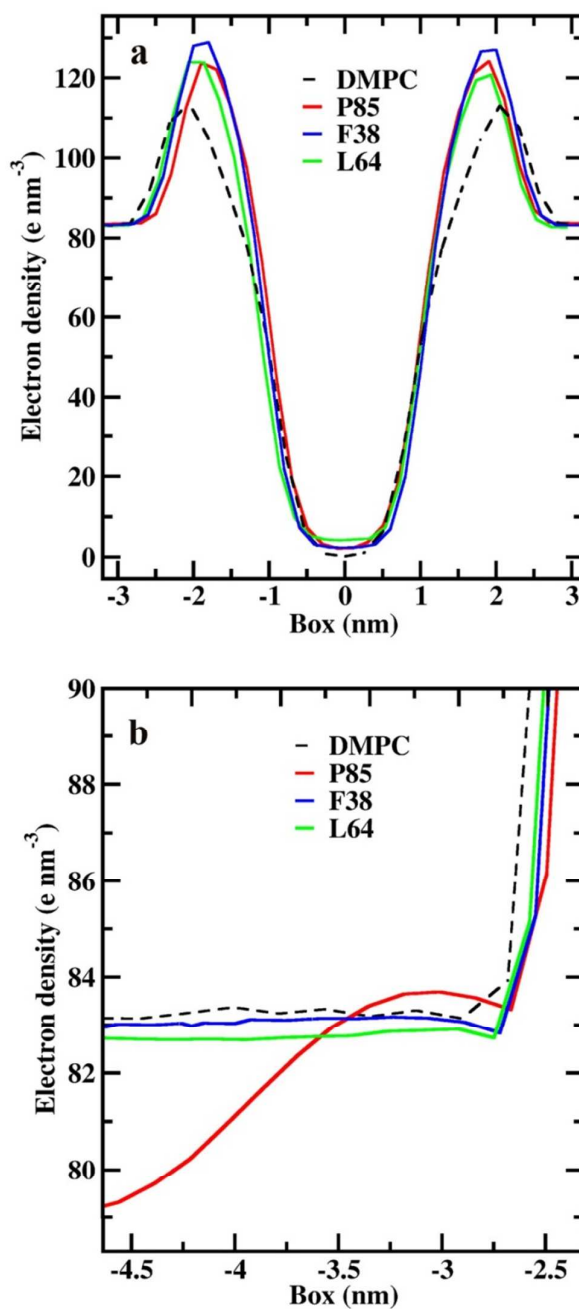


Figure 8. Snapshots from the simulations of five chains of P85 or L64 with DMPC bilayer. The snapshots are shown from top and side views. For clarity, the PPO blocks are shown in different colors and water molecules are not shown.

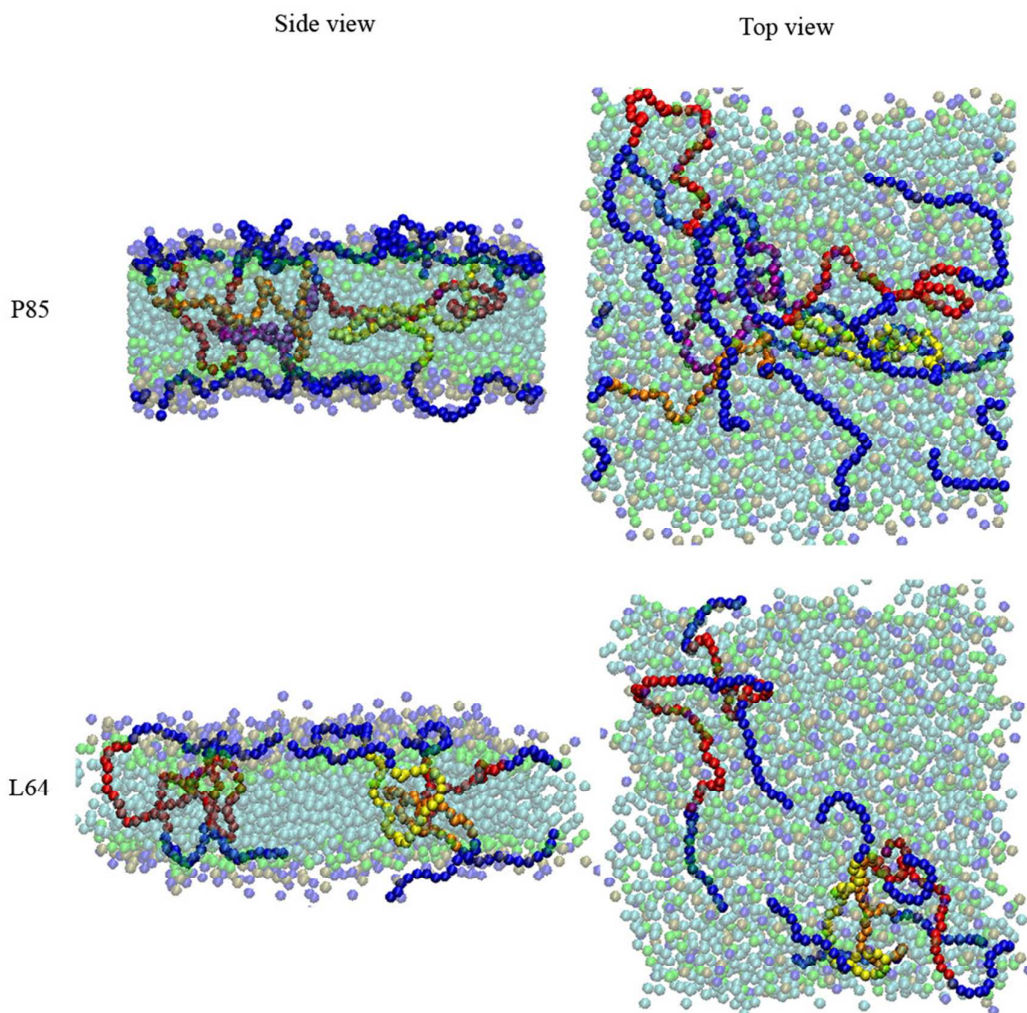


Figure 9. Electronic density profile obtained from the simulations of DMPC bilayer in the presence of five chains of Pluronic. Detail of the membrane region (top) and of the water region (bottom). The DMPC curve contains also the water density.

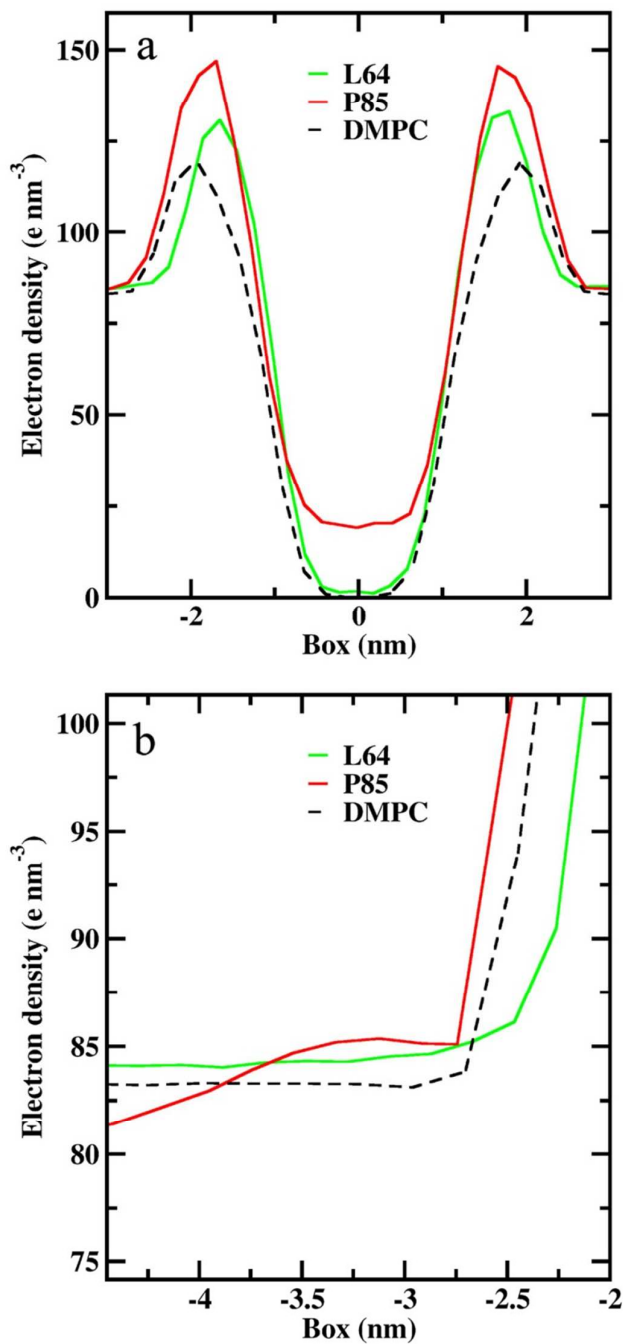


Figure 10. Different simulation timeframes representing the process of interaction of P85 with DMPC bilayer and in particular the PPO block insertion into tail region of the bilayer. Water is not shown for clarity.

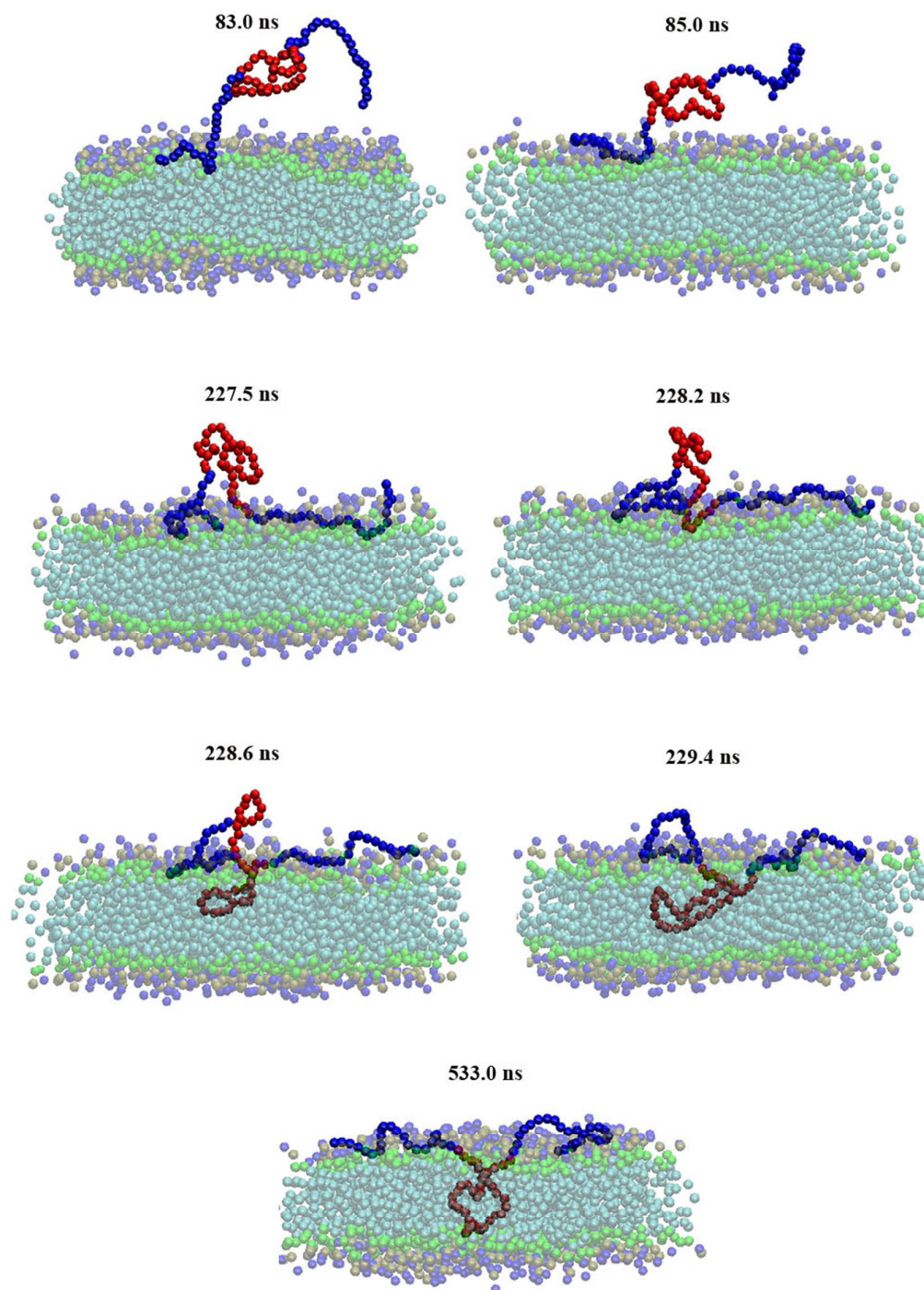


Figure 11. Density profiles from the simulation of L64 or P85 with DMPC bilayer. Density of PEO and PPO blocks in each Pluronic were calculated separately. On the right, the same plots are scaled to better evidence the PPO and PEO density.

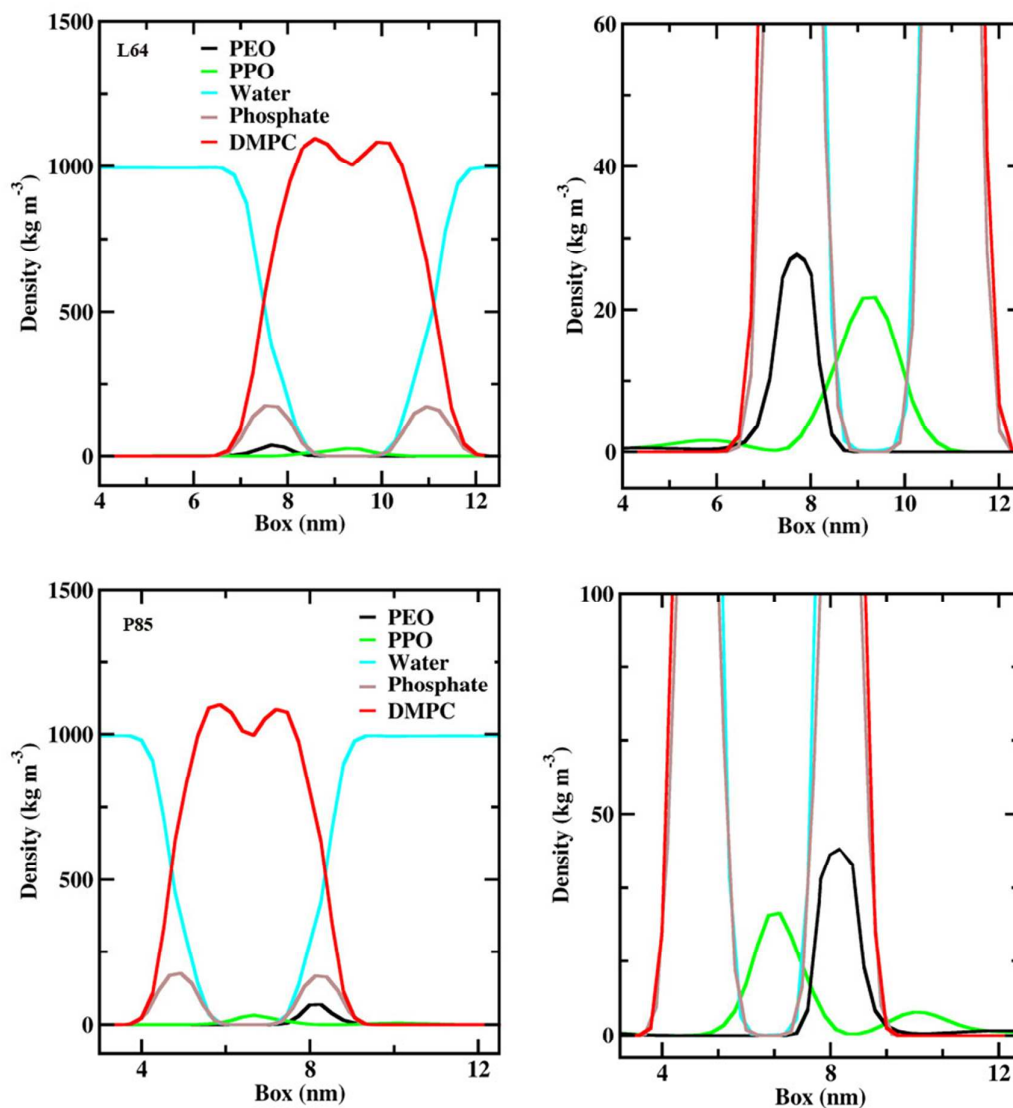
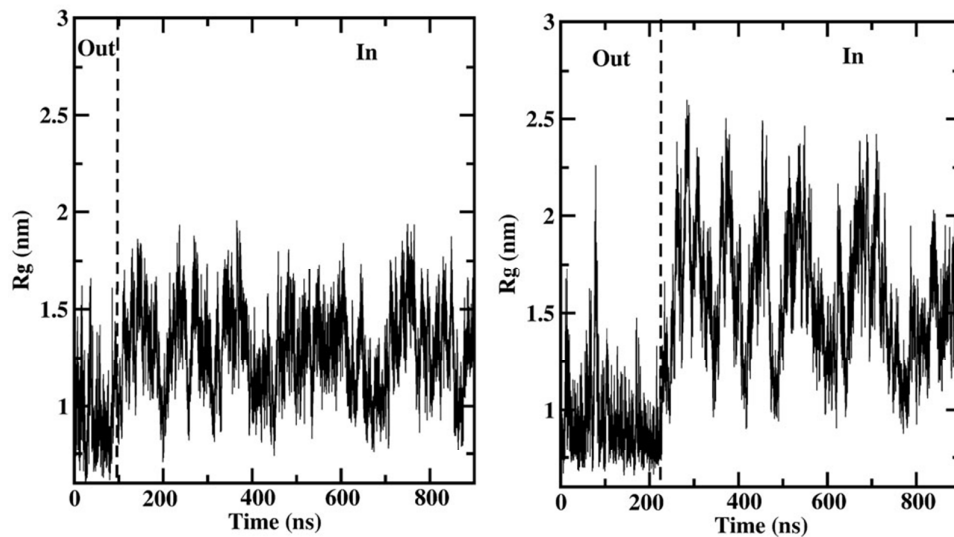


Figure 12. Time series of PPO block R_g vs. time for L64 (left) and P85 (right). Dashed lines indicate the time the time at which PPO block insert completely inside the bilayer.



1
2
3 **Figure 13.** Different simulation timeframes representing the process of interaction of
4 five Pluronics chains located at the beginning of the simulation on the top of the
5 DMPC bilayer. Water is not shown for clarity.
6
7
8
9

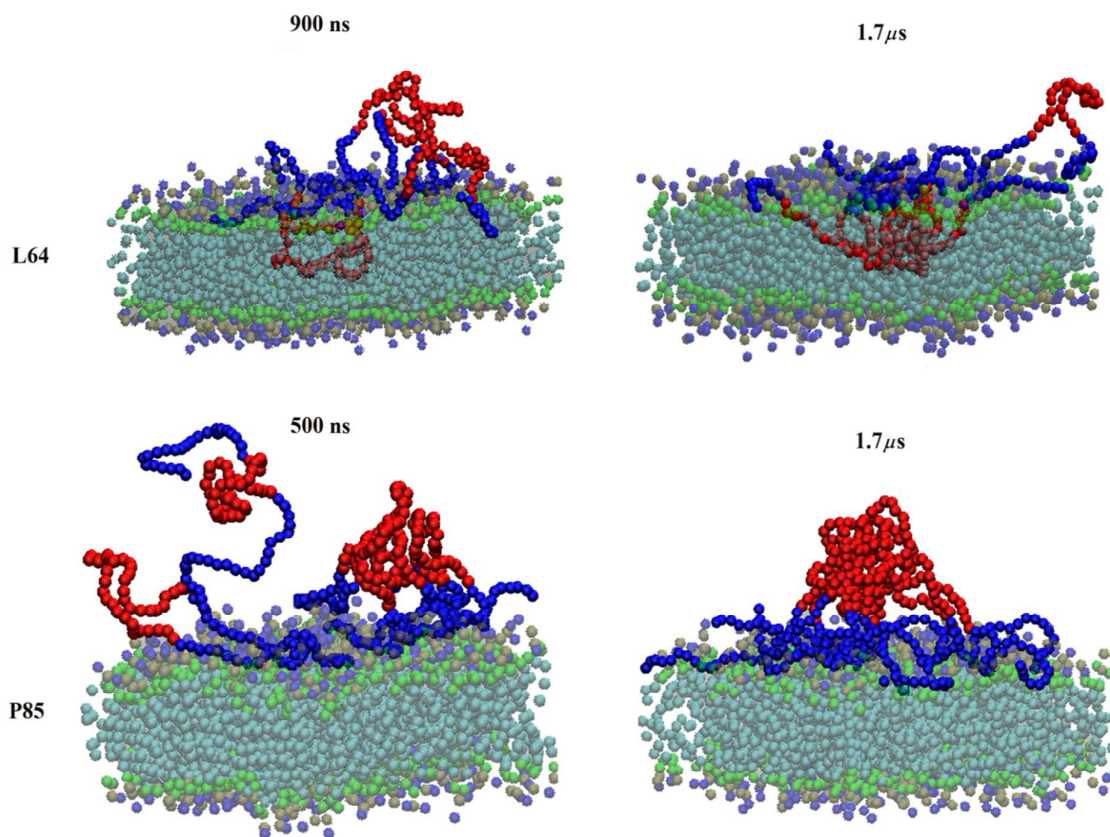
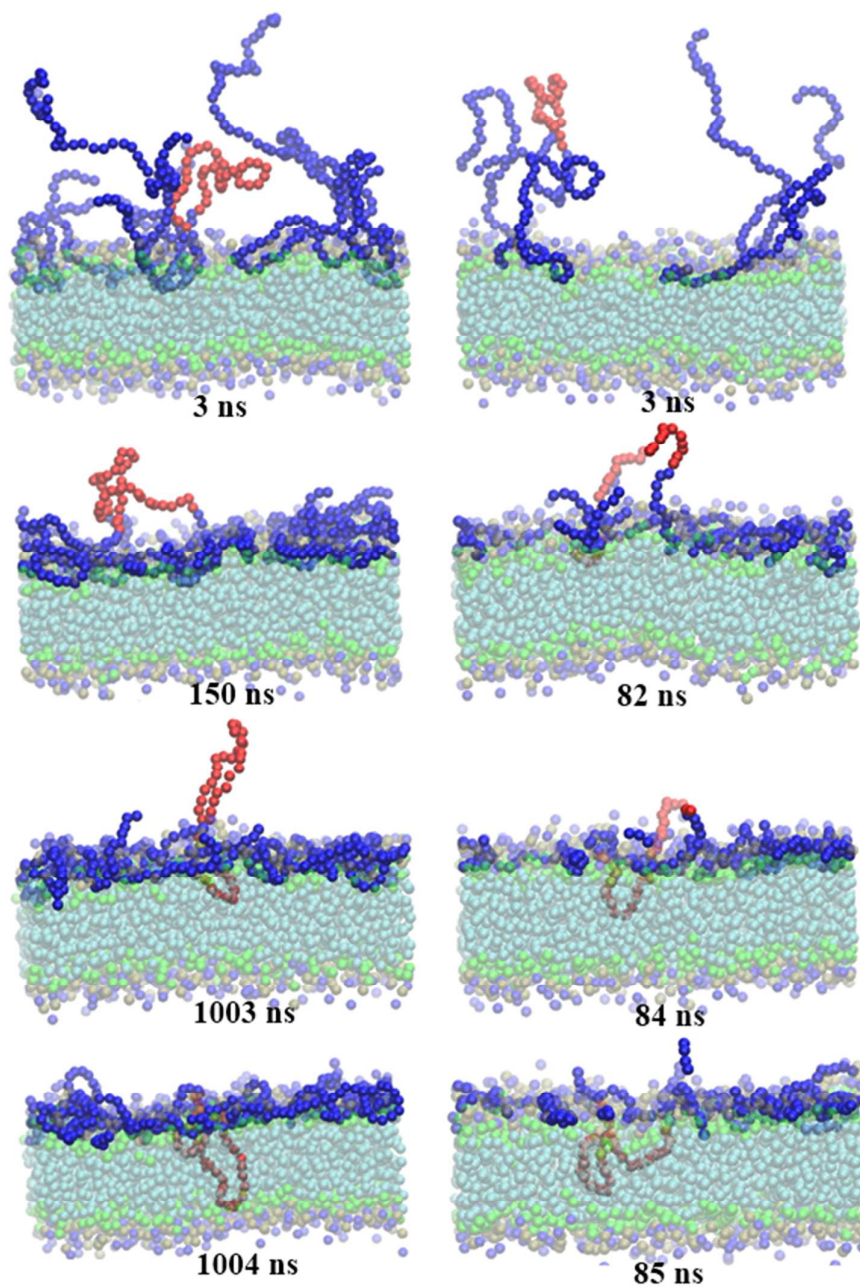


Figure 14. Different simulation timeframes representing the process of interaction of one Pluronic chain plus four PEO chains located at the beginning of the simulation on the top of the DMPC bilayer. In first column snapshots from the P85 and in the second from L64 simulations are reported, respectively. Water is not shown for clarity.



TOC GRAPHIC.

